Optimization of Giant Magnetoimpedance Effect in Magnetic Microwires

Arcady Zhukov
Dept Materials Physics, Univ. Basque Country, UPV/EHU, 20018 San Sebastian and Ikerbasque, Bilbao Spain
e-mail: arkadi.joukov@ehu.es

Paula Corte-León, Mihail Ipatov, Valentina Zhukova
Department Materials Physics, Univ. Basque Country, UPV/EHU, 20018 San Sebastian, Spain
e-mail: paula.corte@ehu.eus, mihail.ipatov@ehu.eus, valentina.zhukova@ehu.es

Juan Maria Blanco
Department Applied Physics I, Univ. Basque Country, EIG, UPV/EHU, 20018, San Sebastian, Spain
e-mail: juanmaria.blanco@ehu.es

Abstract—**In this work, we present the experimental results of our study of various parameters of the Giant MagnetoImpedance (GMI) effect of magnetic microwires. We observed that the GMI effect and the magnetic softness of microwires can be tailored by controlling the Magnetoelastic anisotropy of as-prepared microwires. On the other hand, the GMI ratio can be optimized selecting appropriate measuring conditions, i.e., the measuring frequency.**

Keywords- giant magnetoimpedance effect; magnetic microwires; magnetic softness.

I. INTRODUCTION

Studies of the Giant MagnetoImpedance (GMI) effect have attracted considerable attention since its rediscovery in 1994 in amorphous wires [1][2]. It is worth noting that the first report on the change of impedance in permalloy wires was published in 1936 [3]. However, GMI studies become one of the most attractive topics of applied magnetism owing to the development of amorphous magnetically soft wires [4]-[8].

The main technological interest in the GMI effect is related to one of the largest sensitivities to a magnetic field (up to 10 %/A/m) among non-cryogenic effects [4]-[8]. Such features of the GMI effect make it quite attractive for development of high performance sensors allowing detection of low magnetic fields and mechanical stresses [9]-[14].

The most common quantity for the characterization of the GMI effect is the GMI ratio, $\Delta Z/Z$, defined as:

$$\Delta Z/Z = [Z(H) - Z(H_{max})] / Z(Hmax) \quad (1)$$

where H is the applied axial Direct Current (DC)-field with a maximum value, H_{max}, up to a few kA/m.

The value of the GMI ratio and its magnetic field dependence are determined by the type of magnetic anisotropy: for achievement of high GMI ratio, the high circumferential magnetic permeability is essentially important [7][8]. Magnetic wires with circumferential easy axis exhibit double-peak magnetic field dependence of the real component of wire impedance (and, consequently, of the GMI ratio). Magnetic wires with longitudinal easy axis present monotonic decay of the GMI ratio with increasing axial magnetic field with GMI ratio maximum at zero magnetic field [7][8]. The highest GMI ratio up to 650% is reported for amorphous microwires [15]-[17]. However, theoretically predicted maximum GMI ratio is about 3000% (i.e., a few times larger than the GMI ratio values reported experimentally) [18]. Additionally, the theoretical minimum of the skin depth is about 0.3 μm [18][19].

The main features of the GMI effect have been successfully explained in terms of classical electrodynamics considering the influence of a magnetic field on the penetration depth of an electrical current flowing through the magnetically soft conductor [1][2]. High circumferential permeability typically observed in Co-rich amorphous wires with nearly-zero magnetostriction coefficient is essential for the observation of a high GMI ratio [1][2][4]-[6]. However, similarly to the magnetic permeability, the GMI effect has a tensor character [4]-[6][20]-[22]. The off-diagonal component of MagnetoImpedance (MI) can present anti-symmetrical magnetic field dependence with a linear region quite suitable for magnetic sensors applications [20]-[22].

One of the tendencies in modern GMI sensors is the size reduction. It must be underlined that the diameter reduction must be associated with the increasing of the optimal GMI frequency range: a tradeoff between dimension and frequency is required in order to obtain a maximum GMI effect [4]-[6][23]. Additionally, the GMI effect at microwave frequencies has been described considering the analogy between the GMI and the ferromagnetic resonance [4]. Consequently, development of thin soft magnetic materials required for miniaturization of the sensors and devices requires an extension of the frequency range for the impedance toward the higher frequencies (GHz range).

Depending on the frequency f of the driving AC current I_{ac} flowing through the sample, different GMI regimes can be considered [4]-[6]:

1. Low frequency (1-10 kHz) range when the skin depth is larger than the sample radius (weak skin effect). The impedance changes in this frequency band are related

 ISBN: 978-1-61208-745-0

to a circular magnetization process exclusively and might not be considered as the GMI effect.

2. At the frequency range from 10-100 kHz to 1-10 MHz (where the GMI effect has been first reported and described), the GMI originates basically with the variation of the skin penetration depth of magnetic conductor due to strong changes of the magnetic permeability caused by a DC magnetic field [1][2][4]-[6]. In this frequency band, both domain walls movement and magnetization rotation are considered as to be responsible for the variation of the circular permeability and, hence, to the skin effect.

3. For the MHz band frequencies (from 1-10 MHz to 100-1000 MHz, depending on the geometry of the sample), the GMI effect is also originated by the skin effect of the soft magnetic conductor, i.e., must be attributed to the GMI. However, at these frequencies, the domain walls are strongly damped. Therefore, the magnetization rotation must be considered as responsible for the magnetic permeability change induced by an external magnetic field [1][2][4]-[8].

4. At GHz frequencies, the magnetization rotation is strongly influenced by the gyromagnetic effect. Increasing the frequency, the GMI peaks are shifted to higher magnetic fields values because the sample is magnetically saturated. At this frequency range, strong changes of the sample's impedance have been attributed to the FerroMagnetic Resonance (FMR) [4]-[6][23].

Recently developed magnetic sensors using the GMI effect allow achieving nT and pT magnetic field sensitivity with low noise [10]-[14][24].

Presently, major attention is focused on high frequency (GHz range) GMI applications owing to the development of thin magnetically soft materials and the recent tendency in miniaturization of magnetic field sensors [4]-[6][10]-[14][24].

The aim of this report is to provide recent results on the optimization of soft magnetic properties and of the GMI effect in magnetic microwires.

The rest of the paper is structured as follows. In Section II, we present the description of the experimental techniques, while in Section III, we describe the results on the effect of post-processing on the GMI ratio of studied microwires. We conclude the paper in Section IV.

II. EXPERIMENTAL DETAILS

As already mentioned in the introduction, the GMI effect usually observed in soft magnetic materials phenomenologically consists of the change of the Alternating Current (AC) impedance, $Z = R + iX$ (where R is the real part, or resistance, and X is the imaginary part, or reactance), when submitted to an external magnetic field, H_0.

The electrical impedance, Z, of a magnetic conductor is given by [1][2]:

$$Z = R_{dc}\, krJ_0(kr)/2J_1(kr) \tag{2}$$

with $k = (1 + j)/\delta$, where J_0 and J_1 are the Bessel functions, r is the wire's radius and δ the penetration depth given by:

$$\delta = (\pi\sigma\mu_\phi f)^{-1/2} \tag{3}$$

where σ is the electrical conductivity, f the frequency of the current along the sample, and μ_ϕ the circular magnetic permeability assumed to be scalar. The DC applied magnetic field introduces significant changes in the circular permeability, μ_ϕ. Therefore, the penetration depth also changes through and finally results in a change of Z [1][2].

The GMI ratio, $\Delta Z/Z$, has been evaluated considering (1).

In ferromagnetic materials with high circumferential anisotropy (the case of magnetic wires), the magnetic permeability possesses tensor nature and the classic form of impedance definition is not valid. The relation between the electric field, e, (which determines the voltage) and the magnetic field, h, (which determines the current) is defined through the surface impedance tensor, $\hat{\varsigma}$, [20]-[22][25]:

$$e = \hat{\varsigma} h \quad \text{or} \quad \begin{Bmatrix} e_z = \varsigma_{zz} h_\varphi - \varsigma_{z\varphi} h_z \\ e_\varphi = \varsigma_{\varphi z} h_\varphi - \varsigma_{\varphi\varphi} h_z \end{Bmatrix} \tag{4}$$

The circular magnetic fields h_φ are produced by the currents i_w running through the wire. At the wire surface $h_z = i/2\pi r$, where r is the wire radius. The longitudinal magnetic fields h_z are produced by the currents i_c running through the exciting coil, $h_z = N_1 i_c$, where N_1 is the exciting coil number of turns. Various excitation and measurement methods are required to reveal the impedance matrix elements. The longitudinal and circumferential electrical field on the wire surface can be measured as voltage drop along the wire, v_w, and voltage induced in the pickup coil, v_c, wound on it [20]-[22][25].

$$v_w \equiv e_z l_w = (\varsigma_{zz} h_\varphi - \varsigma_{z\varphi} h_z) l_w \tag{5}$$

$$v_c \equiv e_\varphi l_t = (\varsigma_{\varphi z} h_\varphi - \varsigma_{\varphi\varphi} h_z) l_t \tag{6}$$

where l_w is the wire length, $l_t = 2\pi r N_2$ the total length of the pickup coil turns N_2 wounded directly on the wire.

The methods for revealing the different elements of impedance tensor are shown in Figure 1. The longitudinal diagonal component, ς_{zz}, is defined as the voltage drop along the wire and corresponds to the impedance definition in classical model (Figure 1a)

$$\varsigma_{zz} \equiv \frac{v_w}{h_\varphi l_w} = \left(\frac{2\pi a}{l_w}\right)\left(\frac{v_w}{i_w}\right) \tag{7}$$

The off-diagonal components $\varsigma_{z\varphi}$ and $\varsigma_{\varphi z}$ and the circumferential diagonal component $\varsigma_{\varphi\varphi}$ arose from cross

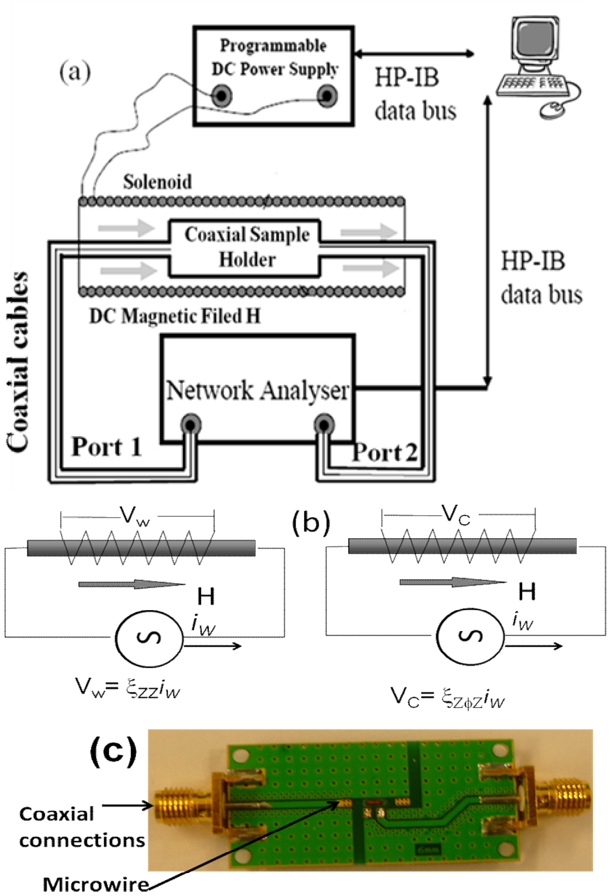

Figure 1. Schematic picture of the experimental set-up for measurements of GMI effect (a), principles for revealing of the diagonal, ς_{zz}, and off-diagonal, $\varsigma_{z\varphi}$, impedance matrix elements (b) and the image of the micro-strip line (c).

sectional magnetization process ($h_\varphi \rightarrow m_z$ and $h_z \rightarrow m_\varphi$) [20]-[22][25].

The use of a specially designed micro-strip sample holder (see Figure 1c) placed inside a sufficiently long solenoid allows measuring of the magnetic field dependence of sample impedance, Z, using a vector network analyzer from the reflection coefficient S_{11} using the expression:

$$Z=Z_0(1+S_{11})/(1-S_{11}) \tag{8}$$

where Z_0=50 Ohm is the characteristic impedance of the coaxial line [26]. The described technique allows measuring of the GMI effect in extended frequency, f, range up to GHz frequencies.

Hysteresis loops have been measured using the fluxmetric method previously described elsewhere [27]. We represent the normalized magnetization, M/M_0 versus the magnetic field, H, where M is the magnetic moment at a given magnetic field and M_0 is the magnetic moment of the sample at the maximum magnetic field amplitude, H_m.

We studied Fe- and Co- rich microwires with metallic nucleus diameters, d, ranging from 10 up to 25 μm prepared using the Taylor-Ulitovsky method described elsewhere [5][8]. The Taylor-Ulitovsky method allows preparation of thinnest metallic wires (with typical diameters of the order of 1 to 30 μm) covered by an insulating glass coating [5][8].

The great advantage of these microwires is that the obtained diameter could be significantly reduced in comparison with the case of amorphous wires produced by the other rapidly quenching methods.

However, in the case of glass-coated microwires, the magnetoelastic anisotropy contribution is even more relevant since the preparation process involves not only the rapid quenching itself, but also simultaneous solidification of the metallic nucleus surrounded by the glass-coating with rather different thermal expansion coefficients [5][8][28]-[30]. The strength of internal stresses, σ_i, is basically affected by three main factors: i) quenching stresses associated to the melt quenching of the metallic alloy; ii) stresses related to the different thermal expansion coefficients of metallic ingot and glass simultaneously solidifying and iii) stresses associated to the drawing of solidifying wire [28]-[30].

In amorphous materials, the magnetocrystalline anisotropy is absent. Therefore, the magnetoelastic anisotropy is the main factor affecting the magnetic properties [5][6].

The magnetoelastic anisotropy, K_{me}, is given as:

$$K_{me} = 3/2\lambda_S\sigma_i \tag{9}$$

where λ_S is the magnetostriction coefficient and σ_i is the internal stresses value [8].

The magnetostriction coefficient, λ_s, value in amorphous alloys can be tailored by the chemical composition [31]-[34]. Generally, Fe-rich compositions present positive λ_s -values (typically $\lambda_s \approx 20 - 40 \times 10^{-6}$), while for the Co-rich alloys, λ_s –values are negative, typically $\lambda_s \approx -5$ to -3×10^{-6}. Vanishing λ_s –values can be achieved in the Co_xFe_{1-x} ($0 \leq x \leq 1$) or Co_xMn_{1-x} ($0 \leq x \leq 1$) systems at x about 0,03 – 0,08 [31]-[34].

However, the internal stresses, σ_i, arise during simultaneous rapid quenching of metallic nucleus surrounding by the glass coating due to the different thermal expansion coefficients. Consequently, the strength of internal stresses can be controlled by glass-coating thickness: the strength of internal stresses increases with the increasing of the glass-coating thickness [28]-[30][35].

III. Experimental Results and Discussion

As mentioned above, the magnitude and the magnetic field dependence of the GMI effect (including off-diagonal components) is intrinsically linked to the magnetic anisotropy [4]-[8]. Magnetoelastic anisotropy is the main source of magnetic anisotropy of amorphous microwires

 ISBN: 978-1-61208-745-0

[4]-[8]. Accordingly, both hysteresis loops, *ΔZ/Z(H)* dependence and maximum value of GMI ratio, $\Delta Z/Z_m$, are affected by λ_s sign and value and by the magnitude of internal stresses, σ_i. The magnetostriction coefficient drastically affects the character of the hysteresis loops of magnetic microwires: i) Co-rich microwires (see Figure 2a for $Co_{77.5}Si_{15}B_{7.5}$) with negative magnetostriction constant ($\lambda_s \approx -5 \times 10^{-6}$) have almost unhysteretic loops with extremely low coercivity, H_c. However, the magnetic permeability of $Co_{77.5}Si_{15}B_{7.5}$ microwire is not high enough since they also present high enough magnetic anisotropy field, H_k. ii) Co-Fe-based microwires with vanishing magnetostriction constant ($Co_{67.1}Fe_{3.8}Ni_{1.4}Si_{14.5}B_{11.5}Mo_{1.7}$, $\lambda_s \approx -10^{-7}$) generally present lower H_k –values and, hence, higher magnetic permeability. iii) Finally, Fe-rich microwires ($Fe_{75}B_9Si_{12}C_4$) with positive magnetostriction constant ($\lambda_s \approx 40 \times 10^{-6}$) present rectangular hysteresis loops and, consequently, low magnetic permeability.

As can be appreciated from Figure 3b, $Co_{67.1}Fe_{3.8}Ni_{1.4}Si_{14.5}B_{11.5}Mo_{1.7}$ microwire presents the highest maximum GMI ratio, $\Delta Z/Z_m$ (about 240% at 500 MHz). Quite low $\Delta Z/Z_m$ –values are observed for $Fe_{75}B_9Si_{12}C_4$ microwire ($\Delta Z/Z_m \approx 15\%$, see Figure. 3c). Moderate $\Delta Z/Z_m$ –values ($\Delta Z/Z_m \approx 120\%$) are observed for $Co_{77.5}Si_{15}B_{7.5}$ microwire (see Figure 3a).

The other difference in *ΔZ/ZH)* dependencies for microwires with different magnetostriction coefficients is the character of *ΔZ/Z(H)* dependencies: for microwire with $\lambda_s>0$ a single maximum *ΔZ/Z(H)* dependence with *ΔZ/Z* maximum at $H=0$ is observed (Figure 3c). However, for

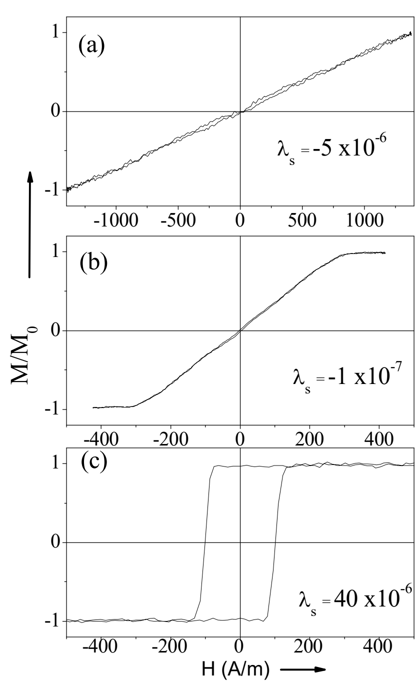

Figure 2. Hysteresis loops of as-prepared $Co_{77.5}Si_{15}B_{7.5}$ (a), $Co_{67.1}Fe_{3.8}Ni_{1.4}Si_{14.5}B_{11.5}Mo_{1.7}$ (b) and $Fe_{75}B_9Si_{12}C_4$ (c) microwires.

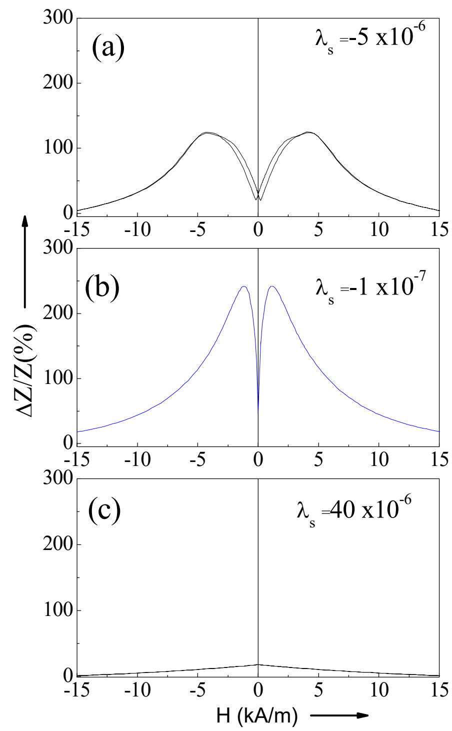

Figure 3. ΔZ/Z(H) dependencies of as-prepared $Co_{77.5}Si_{15}B_{7.5}$ (a), $Co_{67.1}Fe_{3.8}Ni_{1.4}Si_{14.5}B_{11.5}Mo_{1.7}$ (b) and $Fe_{75}B_9Si_{12}C_4$ (c) microwires measured at 500 MHz.

$\lambda_s<0$ double- maximum *ΔZ/Z(H)* dependencies with *ΔZ/Z* maximum at $H=H_m$ are observed (Figures 3b,c).

It is commonly assumed that the H_m -value corresponding to the peaks (maximum ΔZ/Z - value) is linked to the average value of the anisotropy field, H_K, at high frequency values, and to the effective anisotropy distribution in the sample. In this regard, observed *ΔZ/Z(H)* dependencies correlate with hysteresis loops: the highest H_m –value is observed for $Co_{77.5}Si_{15}B_{7.5}$ microwire with the highest H_k –value (see Figure 2a). A single maximum *ΔZ/Z(H)* dependence with *ΔZ/Z* maximum at $H=0$ corresponds to $Fe_{75}B_9Si_{12}C_4$ microwire with axial magnetic anisotropy (Figure 2c).

Such different magnetic anisotropy of microwires with positive and negative magnetostriction is related to the internal stresses distribution, intrinsically related to the fabrication of microwires [4]-[8]. The radial distribution of internal stresses, is calculated considering quenching stresses related to rapid quenching of the metallic alloy from the melt, as well as, complex tensor stresses related with the difference in the thermal expansion coefficients of metal and glass, the axial stresses are the largest ones up to ~ 0.85 *R* (where *R* is the metallic nucleus radius) [8]. Thus, the main volume of the microwire nucleus is under the tensile stresses near the axis of the metallic nucleus. However, closer to the surface the compressive stresses are dominant. Additionally, the strength of internal stresses is determined by the thickness of non-magnetic glass-coating:

the strength of internal stresses increases with the increasing of the glass-coating thickness.

Therefore, as reported earlier [5][8], hysteresis loops and the GMI effect are affected by the ratio $\rho=d/D$, where d is the diameter of metallic nucleus and D-total microwire diameter. Some of the examples are shown in Figure 4, where the hysteresis loops and $\Delta Z/Z(H)$ dependencies of as-prepared $Co_{67}Fe_{3.85}Ni_{1.45}B_{11.5}Si_{14.5}Mo_{1.7}$ microwires with different ρ–ratios are shown.

Consequently, the control of internal stresses by tailoring of the ρ–ratio is the effective method for the GMI ratio tuning.

As mentioned above, the other important parameter for the GMI ratio optimization in magnetic microwires is the frequency. Indeed, the frequency must be high enough in order to have the skin depth lower than the sample radius (strong skin effect).

$\Delta Z/Z(H)$ dependencies measured at different frequencies in as-prepared $Co_{67}Fe_{3.9}Ni_{1.4}B_{11.5}Si_{14.5}Mo_{1.6}$ (d=25.6 μm, D= 26.6 μm) microwires are shown in Figure 5a. This composition at given geometry (d=25.6 μm, D= 26.6 μm, ρ=0.96) present high maximum GMI ratio, $\Delta Z/Z_m$: at the optimal frequency of about 300 MHz, $\Delta Z/Z_m$ ≈550% can be achieved (see Figure 5b). However, thinner (d=10.8 μm) microwire of the same chemical composition at this frequency exhibit $\Delta Z/Z_m$ ≈400% (see Figure 5b). From $\Delta Z/Z_m(f)$ dependence for $Co_{67.7}Fe_{4.3}Ni_{1.6}Si_{11.2}B_{12.4}C_{1.5}Mo_{1.3}$ microwires with d=10.8μm and d=25.6 μm we can appreciate that for $Co_{67.7}Fe_{4.3}Ni_{1.6}Si_{11.2}B_{12.4}C_{1.5}Mo_{1.3}$ microwires with d=10.8μm the optimal frequency is about 700 MHz, at which $\Delta Z/Z_m$ ≈550% can be achieved.

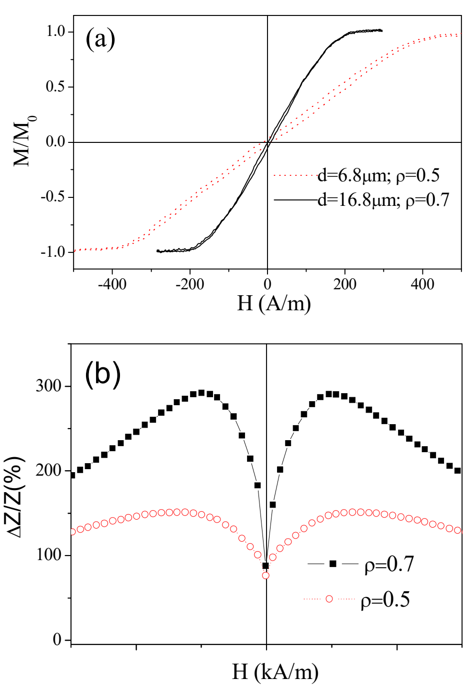

Figure 4. Hysteresis loops (a) and $\Delta Z/Z(H)$ dependencies measured at 500 MHz (b) of as-prepared $Co_{67}Fe_{3.85}Ni_{1.45}B_{11.5}Si_{14.5}Mo_{1.7}$ microwires with different ρ-ratios.

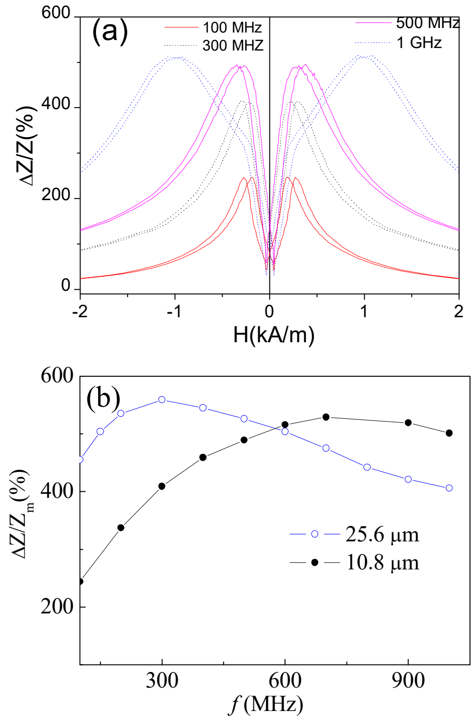

Figure 5. $\Delta Z/Z(H)$ dependencies measured in as-prepared $Co_{67}Fe_{3.9}Ni_{1.4}B_{11.5}Si_{14.5}Mo_{1.6}$ (d=25.6 μm, D= 26.6 μm) microwires (a) and $\Delta Z/Z_m(f)$ dependence for $Co_{67.7}Fe_{4.3}Ni_{1.6}Si_{11.2}B_{12.4}C_{1.5}Mo_{1.3}$ with d=10.8μm, D=13.8μm and d=25.6 μm, D= 26.6 μm microwires.

The aforementioned examples provide the routes for optimization of the GMI effect in Co-rich microwires.

IV. CONCLUSIONS

In this work, we measured the GMI magnetic field, frequency dependencies and hysteresis loops in magnetic microwires produced by the Taylor-Ulitovsky technique.

We observed that the GMI effect and magnetic softness of the microwires are intrinsically related and can be tailored either by controlling the magnetoelastic anisotropy of as-prepared microwires or by controlling their internal stresses and structure by heat treatment. Studies of magnetic properties and the GMI effect of amorphous Co-Fe rich microwires reveal that, by selecting an appropriate chemical composition and geometry, they present GMI effect at GHz frequencies. High GMI effect has been achieved and discussed. The selection of appropriate measuring conditions can be beneficial for optimization of the GMI effect of magnetic microwires.

ACKNOWLEDGMENT

This work was supported by Spanish MCIU under PGC2018-099530-B-C31 (MCIU/AEI/FEDER, UE) and by the Government of the Basque Country under the PIBA 2018-44 project. The authors are grateful for the technical and human support provided by SGIker of UPV/EHU

 ISBN: 978-1-61208-745-0

(Medidas Magnéticas Gipuzkoa) and European funding (ERDF and ESF).

REFERENCES

[1] L. V. Panina and K. Mohri, "Magneto-impedance effect in amorphous wires," Appl. Phys. Lett., vol. 65, pp. 1189-1191, 1994.

[2] R. S. Beach and A. E. Berkowitz, "Giant magnetic-field dependent impedance of amorphous FeCoSiB wire", Appl. Phys. Lett., vol. 64, pp. 3652-3654, 1994.

[3] E. P. Harrison, G. L. Turney, H. Rowe, and H. Gollop, "The electrical properties of high permeability wires carrying alternating current", Proc. R. Soc. Lond. A, vol. 157, pp. 451-479. 1936.

[4] M. H. Phan and H. X. Peng, "Giant magnetoimedance materials: Fundamentals and applications", Prog. Mater. Sci., vol. 53, pp. 323-420, 2008.

[5] A. Zhukov, M. Ipatov, and V. Zhukova, Advances in Giant Magnetoimpedance of Materials, Handbook of Magnetic Materials, ed. K. H. J. Buschow, 24, pp. 139-236 (chapter 2), 2015.

[6] M. Knobel, M. Vazquez, and L. Kraus, Giant magnetoimpedance, Handbook of Magnetic Materials, ed. E. Bruck, 15, pp. 497-563, 2003.

[7] N. A. Usov, A. S. Antonov, and A. N. Lagar`kov, "Theory of giant magneto-impedance effect in amorphous wires with different types of magnetic anisotropy", J. Magn. Magn. Mater., vol. 185, pp. 159-173, 1998.

[8] A. Zhukov et al., "Trends in optimization of giant magnetoimpedance effect in amorphous and nanocrystalline materials", J. Alloys Compd., vol. 727, pp. 887-901, 2017.

[9] K. Mohri, T. Uchiyama, L. P. Shen, C. M. Cai, and L. V. Panina, "Amorphous wire and CMOS IC-based sensitive micro-magnetic sensors (MI sensor and SI sensor) for intelligent measurements and controls", J. Magn. Magn. Mater.,vol. 249, pp. 351-356, 2001.

[10] T. Uchiyama, K. Mohri, and Sh. Nakayama, "Measurement of spontaneous oscillatory magnetic field of Guinea-pig smooth muscle preparation using pico-Tesla resolution amorphous wire magneto-impedance sensor", IEEE Trans. Magn., vol. 47, pp. 3070-3073, 2011.

[11] Y. Honkura, "Development of amorphous wire type MI sensors for automobile use", J. Magn. Magn. Mater., vol. 249, pp. 375-381, 2002.

[12] A. F. Cobeño, A. Zhukov, J. M. Blanco, V. Larin, and J. Gonzalez, "Magnetoelastic sensor based on GMI of amorphous microwire", Sensors Actuat. A-Phys, vol. 91, pp. 95-98, 2001.

[13] S. Gudoshnikov et al., "Highly sensitive magnetometer based on the off-diagonal GMI effect in Co-rich glass-coated microwire", Phys. Stat. Sol. (a), vol. 211 (5) pp. 980–985, 2014.

[14] L. Ding, S. Saez, C. Dolabdjian, L. G. C. Melo, A. Yelon, and D. Ménard, "Development of a high sensitivity giant magneto-impedance magnetometer: comparison with a commercial Flux-Gate", IEEE Sensors, vol. 9 (2), pp. 159-168, 2009.

[15] K. R. Pirota, L. Kraus, H. Chiriac, and M. Knobel, "Magnetic properties and GMI in a CoFeSiB glass-covered microwire", J. Magn. Magn. Mater.,vol. 21, L243-L247, 2000.

[16] A. Zhukov, V. Zhukova, J. M. Blanco, and J. Gonzalez, "Recent research on magnetic properties of glass-coated microwires", J. Magn. Magn. Mater., vol. 294, pp. 182-192, 2005.

[17] P. Corte-León et al., "Engineering of magnetic properties of Co-rich microwires by joule heating", Intermetallics, vol. 105, pp. 92-98, 2019.

[18] L. Kraus, "Theory of giant magneto-impedance in the planar onductor with uniaxial magnetic anisotropy", J. Magn. Magn. Mater., vol. 195, pp. 764-778, 1999.

[19] M. Ipatov, V. Zhukova, A. Zhukov, J. Gonzalez, and A. Zvezdin, "Low-field hysteresis in the magnetoimpedance of amorphous microwires", Phys. Rev. B, vol. 81, p. 134421, 2010.

[20] S. I. Sandacci, D. P. Makhnovskiy, L. V. Panina, K. Mohri, and Y. Honkura, "Off-diagonal impedance in amorphous wires and its application to linear magnetic sensors", IEEE Trans. Magn., vol. 35, pp. 3505-3510, 2004.

[21] P. Aragoneses, A. Zhukov, J. Gonzalez, J. M. Blanco, and L. Dominguez, "Effect of AC driving current on magneto-impedance effect", Sensors Actuat. A-Phys, vol. 81/1-3, pp. 86-90, 2000.

[22] A. S. Antonov, I. T. Iakubov, and A. N. Lagarkov, "Nondiagonal impedance of amorphous wires with circular magnetic anisotropy", J. Magn. Magn. Mater., vol. 187(2) pp. 252–260, 1998.

[23] D. Ménard, M. Britel, P. Ciureanu, and A. Yelon, "Giant magnetoimpedance in a cylindrical conductor", J. Appl. Phys., vol. 84, pp. 2805–2814, 1998.

[24] Y. Honkura and S. Honkura, The Development of a High "Sensitive Micro Size Magnetic Sensor Named as GSR Sensor Excited by GHz Pulse Current", 2018 Progress In Electromagnetics Research Symposium (PIERS — Toyama), Japan, 1–4 August 2018, pp. 324—331.

[25] M. Ipatov, V. Zhukova, J. M. Blanco, J. Gonzalez, and A. Zhukov, "Off-diagonal magneto-impedance in amorphous microwires with diameter 6–10 μm and application to linear magnetic sensors", Phys. Stat. Sol. (a) vol. 205, No. 8, pp. 1779–1782, 2008.

[26] A. Zhukov, A. Talaat, M. Ipatov, and V. Zhukova, "Tailoring the high-frequency giant magnetoimpedance effect of amorphous Co-rich microwires", IEEE Magn. Lett., vol. 6, p. 2500104, 2015.

[27] A. Zhukov, M. Vázquez, J. Velázqez, A. Hernando and V. Larin, "Magnetic properties of Fe-based glass-coated microwires", J. Magn. Magn. Mater. vol. 170, pp. 323-330, 1997.

[28] S. A. Baranov, V. S. Larin, and A. V. Torcunov, Technology, "Preparation and properties of the cast glass-coated magnetic microwires", Crystals, vol. 7 p. 136, 2017.

[29] H. Chiriac and T. A. Óvári, "Amorphous glass-covered magnetic wires: preparation, properties, applications", Progr. Mater. Sci., vol. 40 (5) pp. 333-407, 1996.

[30] A. Zhukov et al., "Ferromagnetic resonance and structure of Fe-based glass-coated microwires", J. Magn. Magn. Mater., vol. 203, pp. 238-240, 1999.

[31] G. Herzer, Amorphous and nanocrystalline soft magnets, in Proceedings of the NATO Advanced Study Institute on Magnetic Hysteresis in Novel Materials, Mykonos, Greece, 1-12 July 1996, ed. George C. Hadjipanayis, NATO ASI Series (Series E: Applied Sciences) vol. 338, pp. 711-730. Kluwer Academic Publishers (Dordrecht/Boston/London) 1997.

[32] A. Zhukov et al., "Magnetostriction of Co-Fe-based amorphous soft magnetic microwires", J. Electr. Mater., vol. 45 (1) pp. 226-234, 2016.

[33] Y. Konno and K. Mohri, "Magnetostriction measurements for amorphous wires", IEEE Trans. Magn., vol. 25, pp. 3623-3625, 1989.

[34] K. Mohri, F.B. Humphrey, K. Kawashima, K. Kimura, and M. Muzutani, "Large Barkhausen and Matteucci effects in FeCoSiB, FeCrSiB, and FeNiSiB amorphous wires", IEEE Trans. Magn., vol. 26, pp. 1789-1781, 1990.

[35] H. Chiriac, T.A. Ovari, and A. Zhukov, "Magnetoelastic anisotropy of amorphous microwires", J. Magn. Magn. Mater. vol. 254-255, pp. 469-471, 2003.